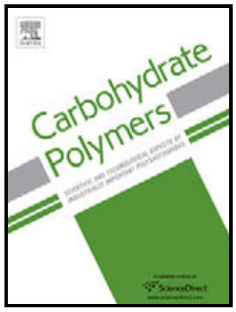

Title: Physical characterisation of high amylose maize starch and acylated high amylose maize starches

Author: Ya-Mei Lim Pamela Hoobin DanYang Ying Iko Burgar Paul R. Gooley Mary Ann Augustin

PII: S0144-8617(14)00978-3
DOI: http://dx.doi.org/doi:10.1016/j.carbpol.2014.09.068
Reference: CARP 9326

To appear in:

Received date: 27-11-2013
Revised date: 9-9-2014
Accepted date: 18-9-2014

Please cite this article as: Lim, Y.-M., Hoobin, P., Ying, D. Y., Burgar, I., Gooley, P. R., and Augustin, M. A.,Physical characterisation of high amylose maize starch and acylated high amylose maize starches, *Carbohydrate Polymers* (2014), http://dx.doi.org/10.1016/j.carbpol.2014.09.068

Physical characterisation of high amylose maize starch and acylated high amylose maize starches

Ya-Mei Lim[1,2,3], Pamela Hoobin[4], DanYang Ying[1], Iko Burgar[4], Paul R Gooley[*,2,3], Mary Ann Augustin[1]

[1]CSIRO Preventative Health National Research Flagship & Animal, Food and Health Sciences, 671 Sneydes Road, Werribee, Vic 3030, Australia

[2]Department of Biochemistry and Molecular Biology, The University of Melbourne, Parkville, Vic 3010, Australia

[3]The Bio21 Molecular Science and Biotechnology Institute, The University of Melbourne, Parkville, Vic 3010, Australia

[4]CSIRO Manufacturing & Materials Technology, Private Bag 33, Clayton South MDC, Clayton South, Victoria 3169, Australia

* Corresponding author

Paul R. Gooley

Department of Biochemistry and Molecular Biology,

The University of Melbourne, Parkville, Vic 3010, Australia.

Tel.: +61 3 834 42273 Email: prg@unimelb.edu.au

Keywords: high amylose maize starch; NMR; Dynamic Vapour Sorption; digestibility; dynamics

List of abbreviations

a_w water activity

CPMG Carr-Purcell-Meiboom-Gill

$D_{4,3}$ mean particle size

DS degree of substitution

EMC equilibrium moisture content

G specific gravity

DVS dynamic vapour sorption

FID free induction decay

HAMS high amylose maize starch

HAMSA acetylated high amylose maize starch

HAMSP propionated high amylose maize starch

HAMSB butyrylated high amylose maize starch

M_o monolayer moisture content

T_2 spin-spin relaxation time

T_1 spin-lattice relaxation time

Highlights

- Heat-induced retrogradation leads to irreversible reduced water interaction abilities
- Particle size is not predictive of water interaction due to internal channel pores
- Complex relationship between starch retrogradation, sizing and water interaction

Abstract

The particle size, water sorption properties and molecular mobility of high amylose maize starch (HAMS) and high amylose maize starch acylated with acetate (HAMSA), propionate (HAMSP) and butyrate (HAMSB) were investigated. Acylation increased the mean particle size ($D_{4,3}$) and lowered the specific gravity (G) of the starch granules with an inverse relationship between the length of the fatty acid chain and particle size. Acylation of HAMS with fatty acids lowered the monolayer moisture content with the trend being HAMSB < HAMSA < HAMSP < HAMS, showing that the decrease is affected by factors other than the length of the fatty acid chain. Measurement of molecular mobility of the starch granules by NMR spectroscopy with Carr-Purcell-Meiboom-Gill (CMPG) experiments showed that T_2 long was reduced in acylated starches and that drying and storage of the starch granules further reduced T_2 long. Analysis of the Free Induction Decay (FID) focussing on the short

components of T_2 (correlated to the solid matrix), indicated that drying and subsequent storage resulted in alterations of starch at $0.33a_w$ and that these changes were reduced with acylation. *In vitro* enzymatic digestibility of heated starch dispersions by bacterial α-amylase was increased by acylation (HAMS < HAMSB < HAMSP ≤ HAMSA) showing that the trend was not related to the length of the fatty acid chain. Digestibility was enhanced with an increase in particle size, or decrease in G, and inversely proportional to the total T_2 signal. It is suggested that both external surface area and an internal network of pores and channels collectively influence the digestibility of starch.

1. Introduction

As a major source of energy for humans and animals, starch that is used in the production of food products and animal feed is often supplied in its dehydrated form to prevent spoilage during transport. High amylose maize starch (HAMS) and high amylose maize starch acylated with acetate (HAMSA), propionate (HAMSP) and butyrate (HAMSB) increase degradative resistance by mammalian enzymes and help to deliver health promoting short chain fatty acid (SCFA) to the host gut (Clarke et al., 2011). To understand the metabolism of the starches by gut microbiota, we previously investigated the breakdown of HAMS and the three modified HAMS by monocultures of bifidobacteria, ruminococcus and faecalibacteria. The starches were differentially degraded with HAMSA being readily degraded while HAMS and HAMSB the least (Lim, Barnes, et al., 2014). This trend is consistent with the notion that the butyl group of HAMSB lies parallel to the glucosyl units whereas the acetyl group of HAMSA lie perpendicular (Lopez-Rubio, Clarke, Ben, Topping & Gilbert, 2009), thus making HAMSA more open and accessible by enzymes. Similar packing was implied in investigations of the hydrodynamic radii of solubilised fractions for these same four starches (Lim, Yao, et al., 2014). While starch structural properties are widely acknowledged to be associated with starch digestion, processing, stability and storage (Chanvrier, Uthayakumaran, Appelqvist, Gidley, Gilbert & Lopez-Rubio, 2007; Shrestha et al., 2012; Zhou, Chung, Kim & Lim, 2013), this area generally remains understudied particularly for high amylose esterified starches.

Techniques such as Fourier transform infrared spectroscopy, neutron scattering, dynamic vapour sorption (DVS), differential scanning calorimetry and nuclear magnetic resonance (NMR) spectroscopy have been used to elucidate the physio-chemical properties of starch

and the role and behaviour of water in food (Choi & Kerr, 2003; Enrione, Hill & Mitchell, 2007; Zeng, Li, Gao & Ru, 2011). Factors such as the composition of the starch, treatments applied during food processing and conditions of storage, all impact on the interactions between water and the starch molecules (Åkerberg, Liljeberg & Björck, 1998; Lewicki, 2004; Svihus, Uhlen & Harstad, 2005). The interactions between water and biopolymer molecules such as starch have a significant influence on biopolymer functionality (Hermansson & Svegmark, 1996). Despite extensive knowledge about the fundamental properties of starch, the ability to predict starch interactions and functionality remain a challenge to the food and starch industry (Copeland, Blazek, Salman & Tang, 2009).

In this study, HAMS and the three acylated HAMS were examined to assess the impact that acylation has on specific gravity (G), particle size and the effect of dry heat treatment and storage on water sorption in the starch molecules. Additionally, we examined the *in vitro* enzymatic digestibility of heated starch dispersions by bacterial α-amylase. The interactions between starch and water were examined using DVS and water mobility was assessed by T_2 distribution profiles using ^{1}H NMR spectroscopy using both Carr-Purcell-Meiboom-Gill (CPMG) and Free Induction Decay (FID) investigations. The relationship between particle size and water-starch interactions on the enzymatic digestibility of starch was assessed.

2. Materials and methods

2.1 Starch material. HAMS, produced by Ingredion (New Jersey, USA) is an unmodified maize starch that contains approximately 70% amylose. HAMS was used as the base starch to manufacture HAMSA, HAMSP and HAMSB (Ingredion). The extent of acylation of these raw starches is expressed as a degree of substitution (DS), which can be defined as the

123 average number of substitution groups per anhydroglucose unit in starch. DS can be
124 calculated using the following equation:
125 DS = [S]/[B]
126 Where [S] is the concentration of the substituent in the sample and [B] is the concentration
127 of the backbone in monomeric terms. As there are only three hydroxyl groups per glucose
128 unit, the maximum DS value for starch is three. The DS values of HAMSA, HAMSP and
129 HAMSB used in this study are 0.22, 0.20 and 0.20 respectively, as determined by Ingredion.
130 The initial moisture content (% dry basis) of the raw starches range from 10.23 to 11.62%.
131
132 **2.2 Amylose content.** The amylose content of the raw starches were determined by their
133 iodine binding capacity using a modified ampero-metric method (Gerard, Barron, Colonna &
134 Planchot, 2001; Larson, Gilles & Jenness, 1953). 100 mg (±10 %) of dry starch was solubilised
135 in 3 ml of 1 N KOH for 10 h at 4 °C with occasional mixing. 3 ml of 1 N HCl and 2 ml of H_2O
136 was added to neutralise the starch solution. 1 ml samples containing diluted starch in the
137 range of 0.5-1 mg and 100 µl of iodine solution (Grams Iodine, Sigma-Aldrich) was prepared
138 and their optical density at 620 nm measured. The amylose content was determined against
139 a standard curve of pure amylose (soluble starch, Sigma Aldrich).
140
141 **2.3 Scanning electron microscopy.** The morphology of the dried starch samples were
142 examined using a field emission scanning electron microscope (SEM) (Quanta; Fei Company,
143 Hillsboro, Oregon, U.S.A.) at 10kV. Raw starch powders were mounted on a stud and coated
144 with gold prior to SEM examination. The detectors used for the SEM observation were an
145 Everhart Thornley detector.
146

147 **2.4 Size distribution and specific gravities.** Particle size analysis of the raw starches was
148 measured by light scattering using a Malvern Mastersizer 2000 (Malvern Instrument,
149 Malvern, UK). Raw starch granules were dispersed in H_2O (10% w/v) and added into the
150 apparatus circulating cell stirring at 2000 rpm. A general purpose analysis model within the
151 Mastersizer analysis software was used with particle refractive and absorption indices of
152 1.53 and 0.1 respectively, while the refractive index of water as the dispersant was 1.33.
153 Duplicate measurements were carried out for each of the starch preparations. Particle size
154 were obtained and expressed in terms of the mean particle size, $D_{4,3}$.
155
156 The G (mass density of solids to that of water), of the starches was obtained using a 25 ml
157 density bottle (pycnometer) at 25 °C. 2000 mg (±10%) of raw starch was used in the
158 determination with ddH_2O as solvent.
159
160 **2.5 Dynamic vapour sorption.** Vapour sorption properties of the raw starches were
161 determined at 25 °C using a controlled-atmosphere microbalance (Dynamic Vapour Sorption
162 Series 2000, Surface Measurement System Ltd., London, U.K.) housed in a controlled
163 temperature incubator (±0.1 °C) as described previously (Ying, Phoon, Sanguansri,
164 Weerakkody, Burgar & Augustin, 2010). Briefly, a sample (~50 mg) was loaded onto a quartz
165 DVS flat bottom sample pan and pre-equilibrated at 0% RH in a continuous flow of dry air
166 for 1000 min before the sample was ramped to the desired water activity. The mass at the
167 end of this step was used as the dry mass. The sample was then exposed to the following
168 water activity (a_w) (0.05, 0.10, 0.20, 0.30, 0.40, 0.50, 0.60, 0.70, 0.80 and 0.90) using a
169 special automatic operation method with *dm*/*dt* (change in mass/time) mode. The *dm*/*dt*
170 criterion was set at 0.001% for five consecutive minutes and the maximum amount of time

171 at each a_w was set at 500 min. The changes in sample mass as a function of time were
172 recorded by the microbalance. Using this method, equilibrium moisture content (EMC) at
173 each a_w was determined. The monolayer moisture content (M_o) was obtained by fitting the
174 isotherm with Guggenheim-Anderson-De Boer model as previously described (Ying, Phoon,
175 Sanguansri, Weerakkody, Burgar & Augustin, 2010). The moisture isotherm was calculated
176 using DVS Analysis Macro version 6.1. The error of the duplicated sorption isotherms was
177 within 3%.
178
179 **2.6 NMR spectroscopy.** Raw starch samples (non-dried) were placed in glass tubes and
180 equilibrated at a_w 0.33 and 0.70 using saturated solutions of magnesium chloride ($MgCl_2$) or
181 of strontium chloride ($SrCl_2$) in sealed glass desiccators. Additionally, dried raw starch
182 samples were prepared similarly following drying at 100 °C for two hours. Spin-spin
183 relaxation time (T_2) were obtained on a MARAN ULTRA 23 MHz spectrometer (Oxford
184 Instruments, Oxfordshire) using the CPMG technique (Hoobin, Burgar, Zhu, Ying, Sanguansri
185 & Augustin, 2013). The 90° - 180° pulse spacing (τ) in the CPMG sequence was set to 30 µs
186 and a dwell time of 0.5 µs and collected until the signal decayed to baseline. The number of
187 scans used was 32 or 64, selected so that the signal to noise ratio was sufficient. Data were
188 fitted using a double exponential equation in Wavemetrics (Igor) software and obtaining
189 two T_2 time constants. After storage for 6 months in a_w 0.33 and 0.7, additional analysis of
190 the shorter components (correlated to the solid matrix) was carried out using the FID. The
191 FID investigation improved the determination of the shorter T_2 component, which could not
192 be observed accurately using the CPMG method.
193

2.7 Enzymatic digestion by amylase. All starch samples were dispersed in water (0.625 % w/v), aliquot into 8 ml fractions and autoclaved for 15 min at 121 °C. Amylase stock solution (α-amylase from *Bacillus licheniformis*, Sigma-Aldrich) was added to each fraction to make up a final volume of 10 ml, a final enzymatic concentration of 50 U/ml and 0.5 % (w/v) starch and incubated at 37 °C for the duration of the experiment. To quantify residual starch, the sample is centrifuged at 4000 g for 5 mins. The pelleted starch is hydrolysed using 10 % HCl (v/v) at 95 °C and quantified using ^{1}H NMR (Lim, Barnes, et al., 2014) .

3. Results

3.1 Amylose content, shape and size distribution of starch granules. Amylose:amylopectin ratios of the chemically modified starches were not altered significantly by acylation, with the four starches containing 69.33 - 70.81 % amylose (Table 1). All four starches appear similar in size and were generally round or oval with a small percentage being irregular (Figure 1). The micrographs of HAMS display filamentous and rod-like characteristics typical in starches with high-amylose content (Fishman, Cooke, White & Damert, 1995). In contrast, modified HAMS granules appear to be more angular, with bulbous protrusions on the starch surfaces.

The particle size distributions of the raw starch obtained by light scattering (Figure 2) confirms that there was a heterogeneous distribution of particles, with modified HAMS possessing a wider range than HAMS, and the most polydispersed starch being HAMSA. The mean particle size ($D_{4.3}$) of HAMS (12.4 µm) and HAMSB (15.8 µm) were found to be smaller than HAMSP (24 µm) and HAMSA (28.7 µm) with the trend being HAMS < HAMSB < HAMSP < HAMSA. Corn starches are typically in the range of 2-26 µm with commercial corn starch

having a $D_{4,3}$ of 16.9 µm (Hossen, Sotome, Takenaka, Isobe, Nakajima & Okadome, 2011; Vasanthan & Bhatty, 1996).

The polydispersity of modified HAMS, especially HAMSA, suggests a portion of the starch may either be larger due to esterification-induced change or are aggregating. With light scattering, a few large aggregates can skew the distribution towards one that emphasises the size of the large particles. To further investigate other factors that might contribute to the $D_{4,3}$ differences, the G of the starches were measured as this provides insights into esterification-induced alterations to the internal packing of the starch (Table 1). There was no significant difference in G between HAMSA and HAMSP. However, HAMS was found to have the highest G, followed by HAMSB and HAMSA/HAMSP. HAMS is the most dense, with the trend in density being HAMSA, HAMSP < HAMSB < HAMS which is consistent with the observed $D_{4,3}$ values.

3.2 Dynamic vapour sorption. The moisture sorption isotherms of the starches are given in Figure 3. The M_o of the starches are in a range of 7.9 – 8.4 g H_2O/100 g solids with HAMSB (7.9) < HAMSA (8.0) < HAMSP (8.3) < HAMS (8.4), showing that the trend in the decrease in M_o did not parallel the increase in length of the fatty acid chain. The M_o values of HAMS and modified HAMS were lower than reported for potato flour (9.79 g H_2O/100 g solids), wheat flour (9.89 g H_2O/100 g solids) and corn flour (10.27 g H_2O/100 g solids) (Timmermann, Chirife & Iglesias, 2001).

3.3 NMR spectroscopy. The measured T_2 distributions show decaying signals representative of both mobile and less mobile ^1H components in the samples which provide information on

242 the interactions of water with the starch molecules. The T_2 values and distribution of the
243 dried and non-dried starches equilibrated at a_w values of 0.33 and 0.70 after 19 days using
244 the described CPMG sequence (Hoobin, Burgar, Zhu, Ying, Sanguansri & Augustin, 2013) are
245 shown in Figure 4, respectively. While the exact moisture content are not measured for
246 each sample due to the small sample size, moisture uptake was measured by weight change
247 and is given in Table S1 (see supplemental material). The distribution curves showed that T_2
248 long is reduced in acylated starches and that drying and subsequent storage of the starch
249 granules further reduced T_2 long. As the distribution from the CPMG decay (Figure 4) does
250 not enable an accurate determination of the T_2 short and long values, the original data was
251 processed by Igor software with a double exponential fit to obtain T_2 values with better
252 accuracy. Using Igor software two distinct T_2 time constants could be discerned (Table 2)
253 which confirms that T_2 values and % contributions to the signal were decreased by acylation.
254 At 0.33 a_w, a fast-decaying component is characterised with the following T_2 short values:
255 HAMS (294 μs) > HAMSP (112 μs) > HAMSB (81.4 μs) > HAMSA (73.5 μs). The same trend is
256 observed for the slow-decaying component with the following T_2 long values: HAMS (814 μs)
257 > HAMSP (609 μs) > HAMSB (512 μs) > HAMSA (453 μs). At 0.70 a_w, these times became less
258 discerning for the acylation state. While the fast-decaying component shows similar values
259 (T_2 short) to the 0.33 a_w data: HAMS (218 μs) > [HAMSA~HAMSP~HAMSB (97-102 μs)], the
260 slow-decaying data showed an increase in T_2 values (T_2 long): HAMS (1670 μs) >
261 HAMSP~HAMSB (1170-1190 μs) > HAMSA (890 μs). However, in all cases, acylation for the
262 non-dried starches decreases T_2 for both fast and slow-decaying components, suggesting a
263 more rigid structure is formed after acylation.
264

As the CPMG sequence did not allow detection of the very short T_2 component (solid matrix), the FID was used to obtain more accurate estimations of these fast-decaying components after 6 month storage (Table 3). The major findings relating to the effects of acylation on molecular mobility in non-dried starches stored at 0.33 a_w were that (i) the integral of the total T_2 signal of the FID component was reduced in acylated starches compared to the unmodified starch with the order of the total T_2 signal being HAMS > HAMSB > HAMSP > HAMSA and (ii) the contribution of T_2 short of the FID component increased with the length of the fatty acid chain, suggesting that as fatty acid length is increased, there are more immobile components. Long term storage of previously dried starch (100 °C/2 h) at a_w 0.33 caused a shift in T_2 distribution with reduced T_2 long (both contribution and integral value) (Table 3). Furthermore, the % increase in the contribution of T_2 short to the total signal was greatest for HAMS. The lower % increase in the contribution of T_2 short for the acylated starches on storage is consistent with the mobility of starch being reduced with acylation (Adebowale & Lawal, 2003; Lawal, 2004).

3.4 Digestion of heated starch dispersion by α-amylase. Digestion of heated starch dispersion *in vitro* by bacterial α-amylase was tracked over a time period of 27 h as shown in Figure 5. Heated starch dispersions adopt a 'burst granule' state with a fraction being solubilised and the largest of these burst granules being visible to the naked eye as grainy particulates. The hydrodynamic radii of solubilised starch have been shown to follow a trend where HAMSA > HAMSP > HAMSB > HAMS (Lim, Yao, et al., 2014). In the digestion of heated starch dispersions, a similar trend is observed with the order of most rapid to least digested starch determined to be: HAMSA ≥ HAMSP > HAMSB > HAMS. This trend was also observed

in a study of acylated high amylose maize starch digestibility by probiotics and gut bacterial species (Lim, Barnes, et al., 2014).

4. Discussion

Four starches (HAMS, HAMSA, HAMSP and HAMSB) were examined by various techniques to understand their physical characteristics (SEM, G, mean particle sizing), water-starch interactions (DVS and ^{1}H NMR spectroscopy) and their relationship to starch digestibility and mobility during storage.

4.1 Acylation and mean particle size. Increase in angular and irregular granules was observed post-acylation, with the loss of filamentous and rod-like characteristics. The proportion of rod-like granules was previously determined to correlate with amylose content (Fishman, Cooke, White & Damert, 1995; Jiang, Horner, Pepper, Blanco, Campbell & Jane, 2010), although this was not observed in the current study. The bulbous surface of angular granules in modified HAMS also appears to be formed through fusion of smaller granules, as previously observed by (Jiang, Horner, Pepper, Blanco, Campbell & Jane, 2010), which may contribute to the increase in particle size.

Acylation increased the mean particle size with HAMS < HAMSB < HAMP < HAMSA, showing an inverse relationship between acylated group length and particle size. The lack of a direct relationship between the length of the fatty acid chain is contrary to expectations. However, our finding may be rationalised by observations of starch structure from X-ray diffraction studies (Lopez-Rubio, Clarke, Ben, Topping & Gilbert, 2009), which inferred that acylation introduced void spaces in the starch structure. Additionally, longer chain fatty acids (butyric

312 acid) results in smaller void spaces while shorter fatty acids such as acetic acid results in
313 more pronounced structural changes and larger void spaces (Lopez-Rubio, Clarke, Ben,
314 Topping & Gilbert, 2009). This is due to longer chain fatty acids being able to lie parallel to
315 the starch backbone due to their length and flexibility. Comparatively, short fatty acids such
316 as acetic acid extend perpendicular to the starch backbone resulting in greater disruptions
317 to the semi-crystalline nature of starch granules (Lopez-Rubio, Clarke, Ben, Topping &
318 Gilbert, 2009). Support for alteration in internal packing and introduction of void spaces
319 within modified HAMS is also evident in the G of the four starches (Table 1).
320
321 **4.2 Starch alterations on storage.** Drying of starch at 100 °C altered starch-moisture
322 interactions, as evidenced by the changed NMR profiles on starches that had been pre-
323 exposed to heat (100 °C/2 h) before storage at various a_w, using both the CPMG and FID.
324 Using the CPMG sequence, the dried starches had shorter T_2 long illustrating an impeded
325 ability for water to interact with the starch components (Figure 4, Table 2), an effect that is
326 evident after six months. This effect is most pronounced in HAMS while modified HAMS was
327 affected to a lesser degree, suggesting that acylation reduces mobility changes on storage.
328 Confirmation that mobility was reduced in acylated starches was obtained with the FID
329 investigation (Table 3). Others have shown that chemical modification through cross-linking
330 (Liu, Ramsden & Corke, 1999) and acylation of starch alters its mobility and decreases
331 retrogradation (Adebowale & Lawal, 2003; Lawal, 2004).
332
333 **4.3 Relationships between physio-chemical properties and factors affecting starch**
334 **digestibility.** The interaction between water and starch, measured by DVS and NMR are
335 related. The equilibrium water content (EMC) (Figure 3) and T_2 long (Table 3) are linearly

related (but not significantly; Pearson correlation = 0.938, P-value = 0.062) (Figure 6A), but not the multilayer water content (EMC less M_o) (Pearson correlation = -0.693, P-value = 0.307) (Figure 6B). T_2 long has been previously found to be correlated to multilayer water and inactivation rates of encapsulated bacteria (Hoobin, Burgar, Zhu, Ying, Sanguansri & Augustin, 2013; Ying, Phoon, Sanguansri, Weerakkody, Burgar & Augustin, 2010). A similar correlation is not observed in HAMS and modified HAMS, possibly due to the heterogenous structure of starch and differences in particle sizing impeding a straightforward model of water interaction. In this work, HAMSA, which has the largest mean particle size and total T_2 signal, had the greatest digestibility followed by HAMSP, HAMSB and HAMS respectively.

The relationship between the measured physio-chemical properties (i.e. particle size and water relations) and starch digestibility in disrupted granules is complex. Others have found that amylase digestion of starch was reduced as particle size of starch granules was increased (Dhital, Shrestha & Gidley, 2010). They further suggested that digestion rate was essentially determined by external-surface area for potato starch. However, in maize starch, digestibility is often larger than predicted from external surface area, due to the contribution of surface pores and channels to the effective total surface area (Dhital, Shrestha & Gidley, 2010).

The observed effects of particle size and the lack of correlation of mobile water (long T_2) or fatty acid chain length with starch digestion, suggests that other factors have a more significant influence on digestibility of acylated starches. This lack of correlation between fatty acid chain length (i.e. hydrophobicity) is contradictory to studies in α-amylose fragments, which found both glycosidic linkage conformation and hydrophobicity to be

equal factors in water sorption (Fringant, Tvaroska, Mazeau, Rinaudo & Desbrieres, 1995). It is suggested that the disruption to the starch structure caused by the introduction of various fatty acids, as previously observed by others using small angle x-ray scattering (Lopez-Rubio, Clarke, Ben, Topping & Gilbert, 2009), possibly has the overriding influence on the digestibility of the starch.

5. Conclusion

Moisture is an inherent component of many food materials with an important role in the prediction of material properties and food shelf life. Our study shows that acylation with short chain fatty acids alter the physical and chemical properties of starch, though not in accordance to the length of the hydrophobic alkyl chain. Other factors such as openness of the internal structure play a pivotal role. DVS and NMR spectroscopy are valuable tools in understanding starch behaviour and properties in food processing. While heat induced changes and hydrophobicity of acyl chains are contributory, structural alteration appears as the overriding factor affecting acylated starch properties. Systemic studies on other food material are required to determine if this observation extends to other dehydrated material. Importantly, current findings suggest that while butylation of HAMS may aid in delivery of butyric acid to the lower gut (Clarke, et al., 2011), the structural packing of HAMSB is not optimal for bacterial degradation. In contrast, HAMSA adopts a more open structure and is more readily digested suggesting that mixed acylation may produce a more accessible starch that will better function as a delivery vehicle for butyrate.

Acknowledgement

We thank Dr Julie Clarke and Ben Scherer of CSIRO Animal Food and Health Sciences (Adelaide, Australia) for the provision of starches, Sukhdeep Bhail for particle size analysis and Lydia Ong for scanning electron microscopy assistance. The research presented is supported in part by a CSIRO OCE Postgraduate Scholarship and University of Melbourne MIFRS Scholarship.

389

390 **References**

391 Adebowale, K. O., & Lawal, O. S. (2003). Functional properties and retrogradation behaviour
392 of native and chemically modified starch of mucuna bean (Mucuna pruriens). *Journal*
393 *of the Science of Food and Agriculture*, *83*(15), 1541-1546.
394 Åkerberg, A., Liljeberg, H., & Björck, I. (1998). Effects of Amylose/Amylopectin Ratio and
395 Baking Conditions on Resistant Starch Formation and Glycaemic Indices. *Journal of*
396 *Cereal Science*, *28*(1), 71-80.
397 Chanvrier, H., Uthayakumaran, S., Appelqvist, I. A. M., Gidley, M. J., Gilbert, E. P., & Lopez-
398 Rubio, A. (2007). Influence of storage conditions on the structure, thermal behavior,
399 and formation of enzyme-resistant starch in extruded starches. *Journal of*
400 *Agricultural and Food Chemistry*, *55*(24), 9883-9890.
401 Choi, S.-G., & Kerr, W. L. (2003). 1H NMR studies of molecular mobility in wheat starch. *Food*
402 *Research International*, *36*(4), 341-348.
403 Clarke, J. M., Topping, D. L., Christophersen, C. T., Bird, A. R., Lange, K., Saunders, I., &
404 Cobiac, L. (2011). Butyrate esterified to starch is released in the human
405 gastrointestinal tract. *The American journal of clinical nutrition*, *94*(5), 1276-1283.
406 Copeland, L., Blazek, J., Salman, H., & Tang, M. C. (2009). Form and functionality of starch.
407 *Food Hydrocolloids*, *23*(6), 1527-1534.
408 Dhital, S., Shrestha, A. K., & Gidley, M. J. (2010). Relationship between granule size and in
409 vitro digestibility of maize and potato starches. *Carbohydrate Polymers*, *82*(2), 480-
410 488.
411 Enrione, J. I., Hill, S. E., & Mitchell, J. R. (2007). Sorption Behavior of Mixtures of Glycerol and
412 Starch. *Journal of Agricultural and Food Chemistry*, *55*(8), 2956-2963.
413 Fishman, M. L., Cooke, P., White, B., & Damert, W. (1995). Size distributions of amylose and
414 amylopectin solubilized from corn starch granules. *Carbohydrate Polymers*, *26*(4),
415 245-253.
416 Fringant, C., Tvaroska, I., Mazeau, K., Rinaudo, M., & Desbrieres, J. (1995). Hydration of
417 alpha-maltose and amylose: molecular modelling and thermodynamics study.
418 *Carbohydrate Research*, *278*(1), 27-41.
419 Gerard, C., Barron, C., Colonna, P., & Planchot, V. (2001). Amylose determination in
420 genetically modified starches. *Carbohydrate Polymers*, *44*(1), 19-27.
421 Hermansson, A.-M., & Svegmark, K. (1996). Developments in the understanding of starch
422 functionality. *Trends in Food Science & Technology*, *7*(11), 345-353.
423 Hoobin, P., Burgar, I., Zhu, S., Ying, D., Sanguansri, L., & Augustin, M. A. (2013). Water
424 sorption properties, molecular mobility and probiotic survival in freeze dried protein-
425 carbohydrate matrices. *Food & Function*, *4*(9), 1376-1386.
426 Hossen, M. S., Sotome, I., Takenaka, M., Isobe, S., Nakajima, M., & Okadome, H. (2011).
427 Effect of Particle Size of Different Crop Starches and Their Flours on Pasting
428 Properties. *Japan Journal of Food Engineering*, *12*(1), 29-35.
429 Jiang, H., Horner, H. T., Pepper, T. M., Blanco, M., Campbell, M., & Jane, J.-l. (2010).
430 Formation of elongated starch granules in high-amylose maize. *Carbohydrate*
431 *Polymers*, *80*(2), 533-538.
432 Larson, B. L., Gilles, K. A., & Jenness, R. (1953). Amperometric Method for Determining
433 Sorption of Iodine by Starch. *Analytical Chemistry*, *25*(5), 802-804.

Lawal, O. S. (2004). Succinyl and acetyl starch derivatives of a hybrid maize: physicochemical characteristics and retrogradation properties monitored by differential scanning calorimetry. *Carbohydrate Research*, *339*(16), 2673-2682.

Lewicki, P. P. (2004). Water as the determinant of food engineering properties. A review. *Journal of Food Engineering*, *61*(4), 483-495.

Lim, Y. M., Barnes, M. B., Gras, S. L., McSweeney, C., Lockett, T., Augustin, M. A., & Gooley, P. R. (2014). Esterification of high amylose starch with short chain fatty acids modulates degradation by Bifidobacterium spp. *Journal of Functional Foods*, *6*, 137-146.

Lim, Y. M., Yao, S., Gras, S. L., McSweeney, C., Lockett, T., Augustin, M. A., & Gooley, P. R. (2014). Hydrodynamic radii of solubilized high amylose native and modified starches by pulsed field gradient NMR diffusion measurements. *Food Hydrocolloids*, *40*, 16-21.

Liu, H., Ramsden, L., & Corke, H. (1999). Physical Properties of Cross-linked and Acetylated Normal and Waxy Rice Starch. *Starch - StÃ¤rke*, *51*(7), 249-252.

Lopez-Rubio, A., Clarke, J. M., Ben, S., Topping, D. L., & Gilbert, E. P. (2009). Structural modifications of granular starch upon acylation with short-chain fatty acids. *Food Hydrocolloids*, *23*(7), 1940-1946.

Shrestha, A. K., Blazek, J., Flanagan, B. M., Dhital, S., Larroque, O., Morell, M. K., Gilbert, E. P., & Gidley, M. J. (2012). Molecular, mesoscopic and microscopic structure evolution during amylase digestion of maize starch granules. *Carbohydrate Polymers*, *90*(1), 23-33.

Svihus, B., Uhlen, A. K., & Harstad, O. M. (2005). Effect of starch granule structure, associated components and processing on nutritive value of cereal starch: A review. *Animal Feed Science and Technology*, *122*(3-4), 303-320.

Timmermann, E. O., Chirife, J., & Iglesias, H. A. (2001). Water sorption isotherms of foods and foodstuffs: BET or GAB parameters? *Journal of Food Engineering*, *48*(1), 19-31.

Vasanthan, T., & Bhatty, R. S. (1996). Physicochemical Properties of Small- and Large-Granule Starches of Waxy, Regular, and High-Amylose Barleys. *Cereal Chem*, *73*(2), 199-207.

Ying, D. Y., Phoon, M. C., Sanguansri, L., Weerakkody, R., Burgar, I., & Augustin, M. A. (2010). Microencapsulated Lactobacillus rhamnosus GG powders: relationship of powder physical properties to probiotic survival during storage. *Journal of Food Science*, *75*(9), E588-595.

Zeng, J., Li, G., Gao, H., & Ru, Z. (2011). Comparison of A and B Starch Granules from Three Wheat Varieties. *Molecules*, *16*(12), 10570-10591.

Zhou, X., Chung, H.-J., Kim, J.-Y., & Lim, S.-T. (2013). In vitro analyses of resistant starch in retrograded waxy and normal corn starches. *International journal of biological macromolecules*, *55*, 113-117.

477 **Table 1:** Specific gravity and % amylose of HAMS, HAMSA, HAMSP and HAMSB

Starch	HAMS	HAMSA	HAMSP	HAMSB
Specific Gravity	1.50 (0.01)	1.40 (0.03)	1.40 (0.01)	1.44 (0.02)
% amylose	70.81 (1.20)	69.33 (1.16)	70.56 (1.63)	69.47 (0.89)

478

479

480

481 The specific gravity and % amylose of high amylose maize starch (HAMS), acetylated high amylose maize starch (HAMSA), propionated high

482 amylose maize starch (HAMSP) and butyrylated high amylose maize starch (HMASB) were determined in triplicate. (±SEM).

483

484 **Table 2**: T_2 short and T_2 long profiles of dried and non-dried starches after 19 days storage at a_w values of 0.33 and 0.7 using the CPMG decay

485 signal. [a]

486

a_w 0.33		Non-dried				Dried			
		HAMS	HAMSA	HAMSP	HAMSB	HAMS	HAMSA	HAMSP	HAMSB
T_2 short	Time (µs)	294	73.5	112	81.4	93.0	116	171	128
	% contribution	54.3	38.1	35.4	42.1	48.8	70.6%	75.5	70.0
T_2 long	Time (µs)	814	453	609	512	394	409	484	434
	% contribution	45.7	61.9	64.6	57.9	51.2	29.4	24.5	30.0
a_w 0.70		Non-dried				Dried			
		HAMS	HAMSA	HAMSP	HAMSB	HAMS	HAMSA	HAMSP	HAMSB
T_2 short	Time (µs)	218	98.6	102	96.6	192	86.6	80.2	117
	% contribution	20.4	25.8	25.4	28.7	22.0	30.1	28.0	26.5
T_2 long	Time (µs)	1670	890	1170	1190	1150	780	955	969
	% contribution	79.6	74.2	74.6	71.3	78.0	69.9	72.0	73.5

487

488 [a] Error is up to 3% of the measured values. For each starch (HAMS, High amylose maize starch; HAMSA, acetylated high amylose maize starch;

489 HAMSP, propionated high amylose maize starch and HAMSB, butyrylated high amylose maize starch), condition (non-dried, dried) and T_2 time

490 (T_2 short, T_2 long), the mean T_2, the % contribution to the integral of the total T_2 is given.

491

492 **Table 3**: T_2 short and T_2 long profiles of dried and non-dried starches after 6 months of equilibration at a_w values of 0.33 and 0.70 using the FID[a]

a_w 0.33		Non-dried				Dried			
		HAMS	HAMSA	HAMSP	HAMSB	HAMS	HAMSA	HAMSP	HAMSB
T_2 short	Time (µs)	11.2	12.1	12.1	12.1	11.2	11.7	11.7	12.1
	Integral (a.u)	65625	60514	65839	68519	64454	64508	67809	71127
	% contribution	80.8	82.3	83.2	85.0	84.8	86.0	86.9	88.1
T_2 long	Time (µs)	517	536	642	597	360	387	388	387
	Integral (a.u)	15638	12975	13340	12102	11541	10532	10187	9630
	% contribution	19.2	17.7	16.8	15.0	15.2	14.0	13.1	11.9
T_2 total	Total integral	81263	73489	79179	80621	75995	75040	77996	80757
a_w 0.70		Non-dried				Dried			
		HAMS	HAMSA	HAMSP	HAMSB	HAMS	HAMSA	HAMSP	HAMSB
T_2 short	Time (µs)	10.1	10.9	11.3	11.7	10.1	10.9	10.9	11.7
	Integral (a.u)	60345	58673	62527	66128	58140	57322	60743	67837
	% contribution	70.1	69.5	71.5	73.7	71.3	70.0	73.0	74.7
T_2 long	Time (µs)	666	620	691	691	642	598	666	666
	Integral (a.u)	25763	25770	24863	23607	23347	24600	22507	22943
	% contribution	29.9	30.5	28.5	26.3	28.7	30.0	27.0	25.3
T_2 total	Total integral	86108	84443	87390	89735	81487	81922	83250	90780

493

494 [a] Error is up to 3% of the measured values. For each starch (HAMS, High amylose maize starch; HAMSA, acetylated high amylose maize starch;

495 HAMSP, propionated high amylose maize starch and HAMSB, butyrylated high amylose maize starch), condition (non-dried, dried) and T_2 time

496 (T_2 short, T_2 long), the mean T_2, the integral attributed to that T_2 and % contribution to the integral of the total T_2 is given.

Figure Legend

Figure 1: SEM images of (A) HAMS, (B) HAMSA, (C) HAMSP and (D) HAMSB illustrating shape differences and size distributions. Filamentous and rod-like starches are indicated by the open arrows while solid arrows indicate small particles found only in HAMS. Images obtained are of raw starches (prior to dry heat treatment and storage at a_w 0.33 or 0.70). All scale bars = 20 μm.

Figure 2: Deconvoluted light scattering data showing particle size distribution of HAMS and modified HAMS. The distributions for raw starch HAMS (black lines), HAMSA (grey lines), HAMSP (broken grey lines) and HAMSB (broken black lines) illustrate larger particle size of HAMSA and significant overlap between HAMS, HAMSP and HAMSB. Duplicate measurements were obtained prior to dry heat treatment and storage at aw 0.33 or 0.70.

Figure 3: Thermal isotherms of HAMS (◇), HAMSA (□), HAMSP (Δ) and HAMSB (○) illustrating the water sorption properties of raw starches (prior to dry heat treatment and storage at a_w 0.33 or 0.70). Duplicate measurements were obtained with the error of duplicated isotherms within 3 %.

Figure 4: T_2 distribution of dried and non-dried HAMS and modified HAMS after 19 days of storage at a_w of (A) 0.33 and (B) 0.7 as obtained using a CPMG sequence. The y-dimension is off-set for clarity. Poor resolution of T_2 short and T_2 long as seen at a_w 0.33 is discussed in-text.

520 **Figure 5:** Digestion of HAMS (◇), HAMSA (□), HAMSP (Δ) and HAMSB (○) by α-amylase as
521 a function of starting concentration. Error bars represent ±SEM of four independent
522 measurements.

523

524 **Figure 6:** Correlation between T_2 long integral value and (A) equilibrium moisture content
525 and (B) equilibrium moisture content less monolayer moisture content at a_w of 0.33 for
526 HAMS (◇), HAMSA (□), HAMSP (Δ) and HAMSB (○).

527

Figure 1

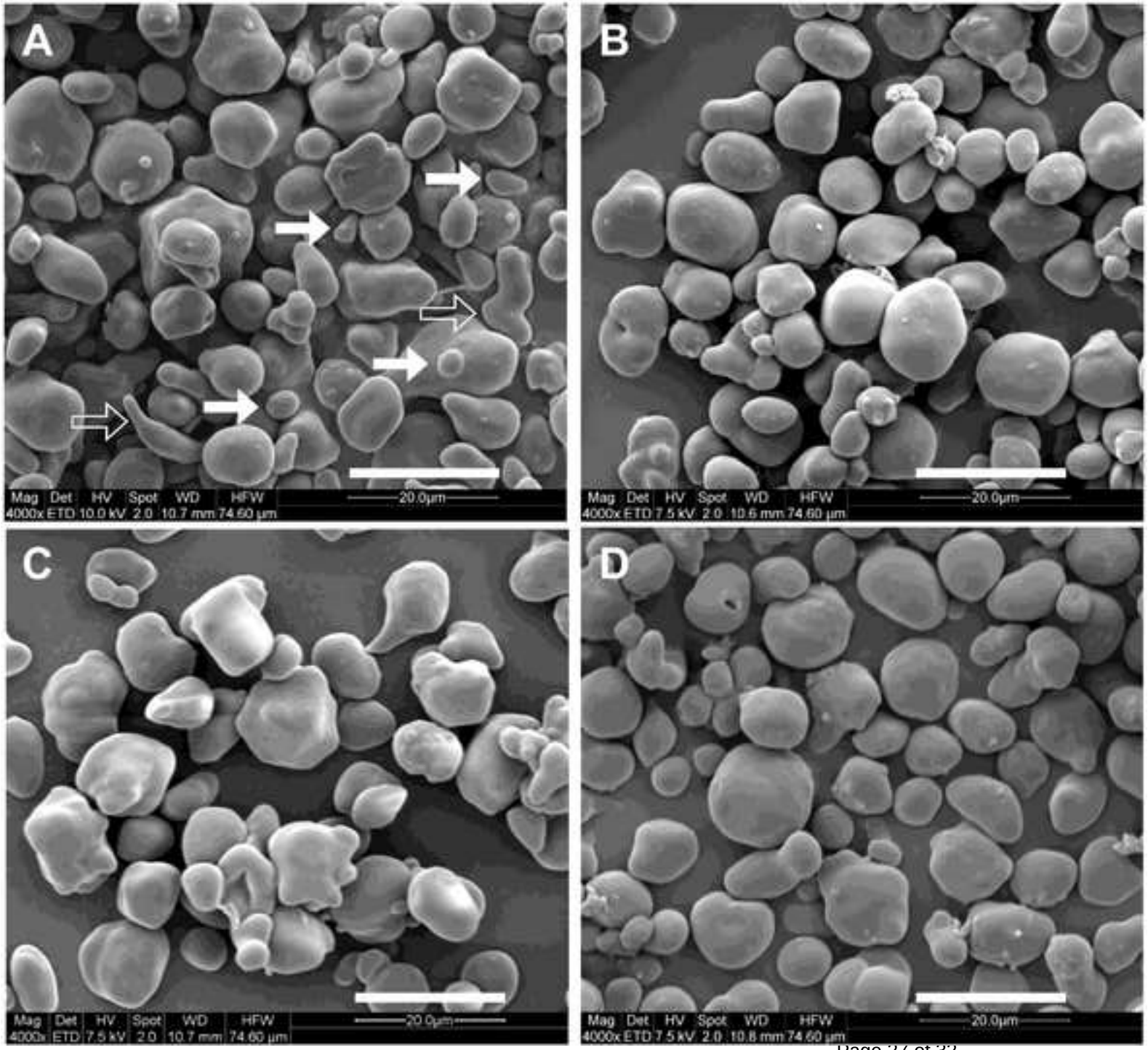
A
Mag Det HV Spot WD HFW
4000x ETD 10.0 kV 2.0 10.7 mm 74.60 µm
20.0µm
B
Mag Det HV Spot WD HFW
4000x ETD 7.5 kV 2.0 10.6 mm 74.60 µm
20.0µm
C
Mag Det HV Spot WD HFW
4000x ETD 7.5 kV 2.0 10.7 mm 74.60 µm
20.0µm
D
Mag Det HV Spot WD HFW
4000x ETD 7.5 kV 2.0 10.8 mm 74.60 µm
20.0µm

Figure 2

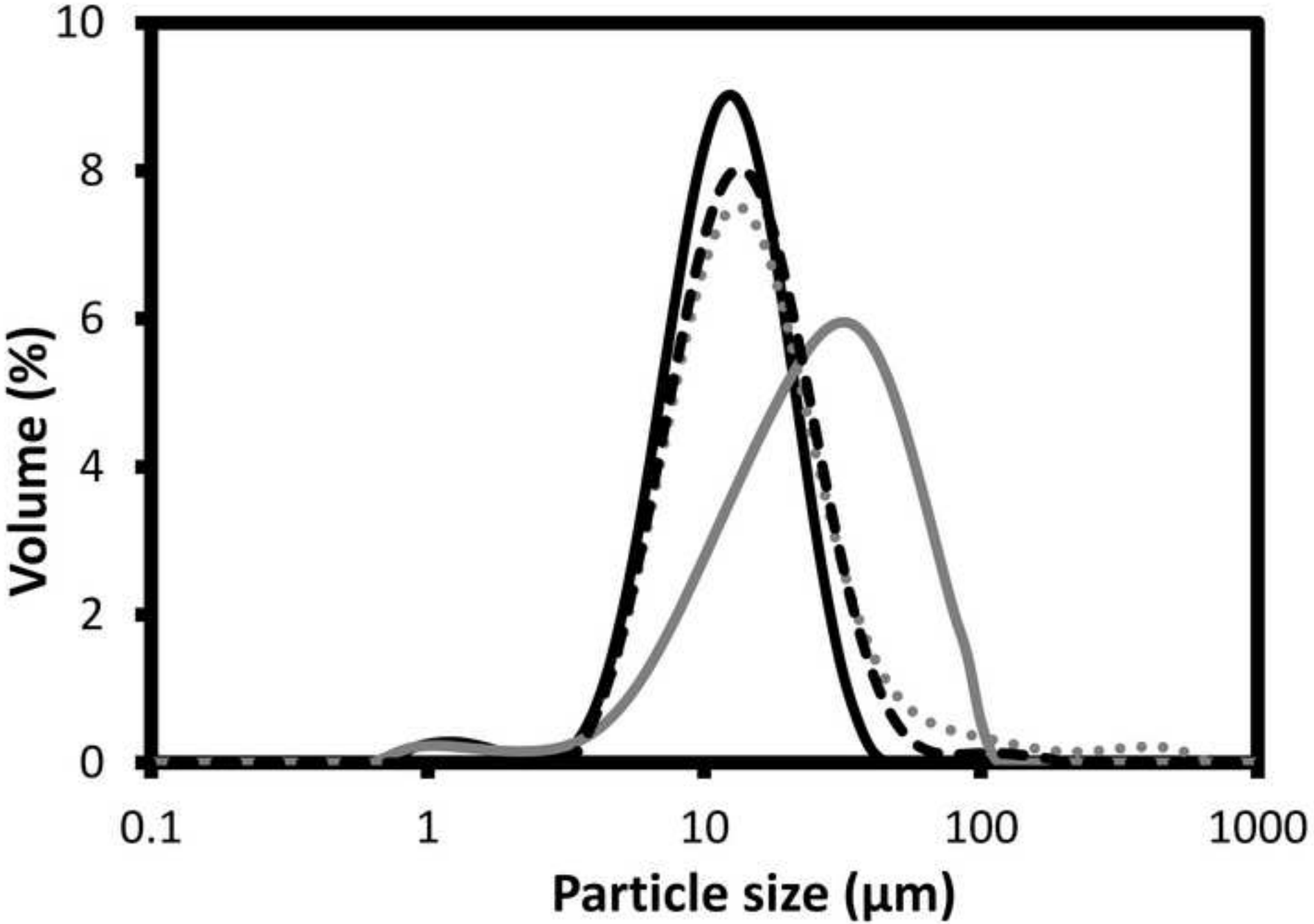

Figure 3

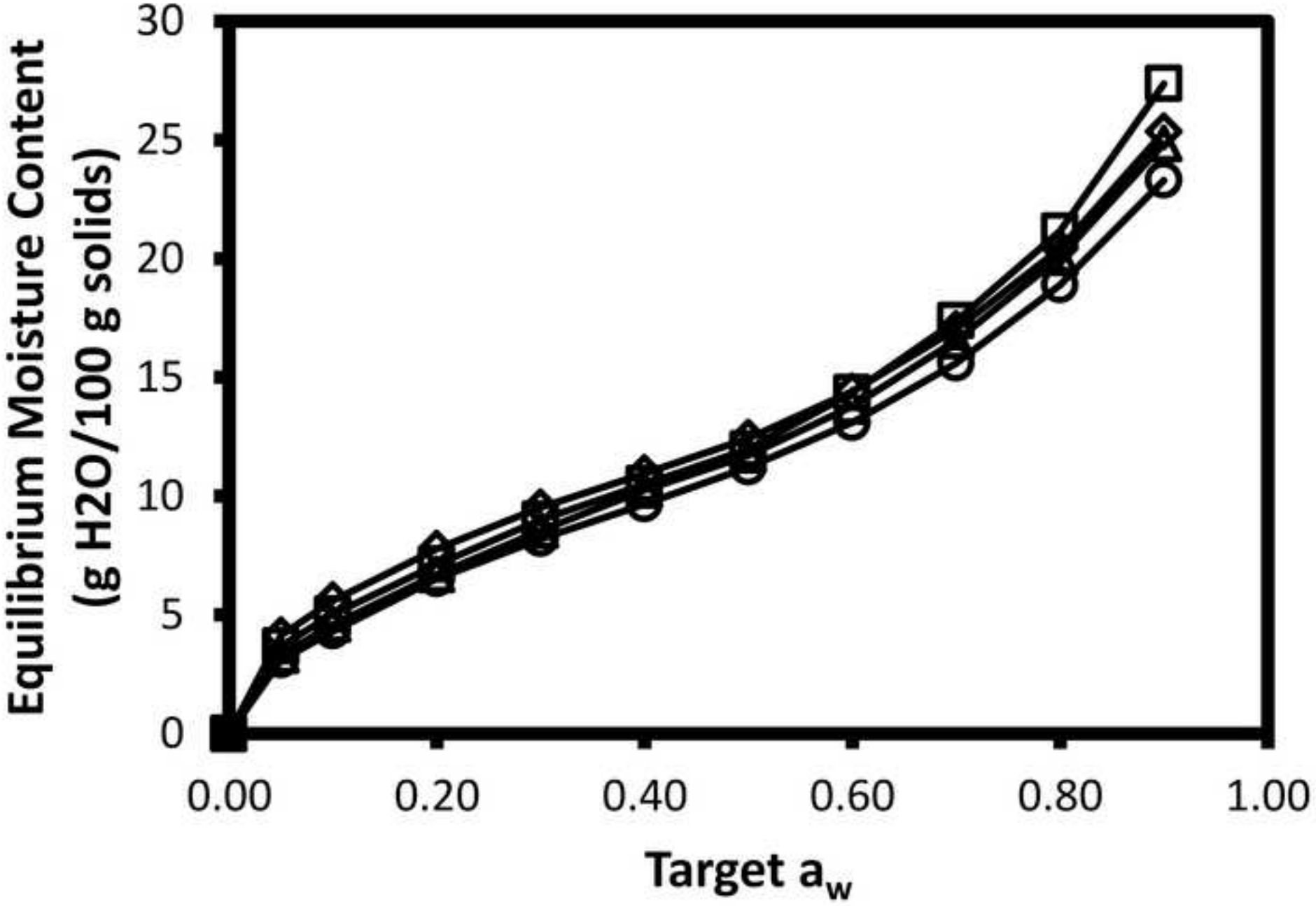
Equilibrium Moisture Content
(g H2O/100 g solids)
30
25
20
15
10
5
0
0.00
0.20
0.40
0.60
0.80
1.00
Target a_w

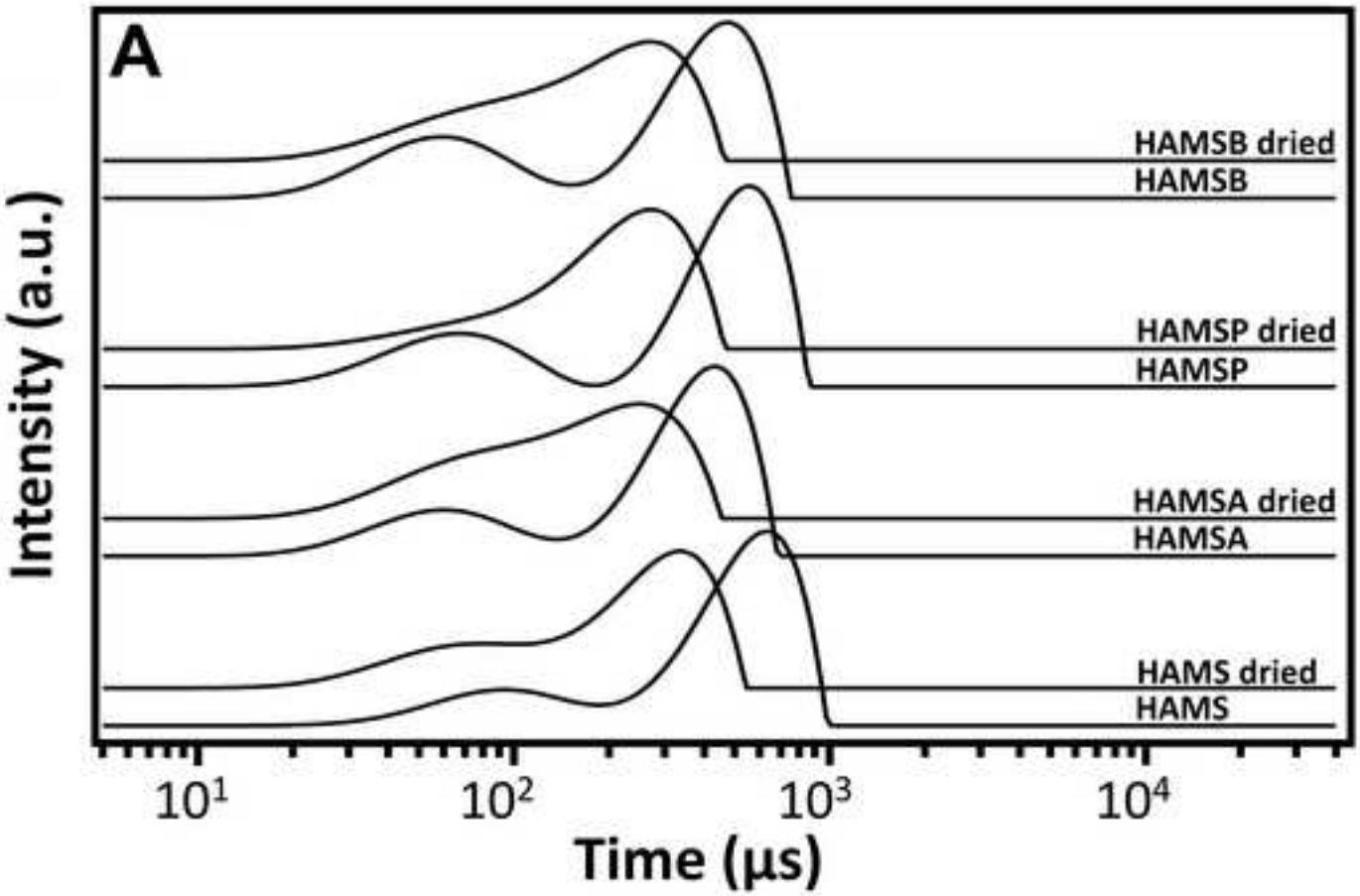

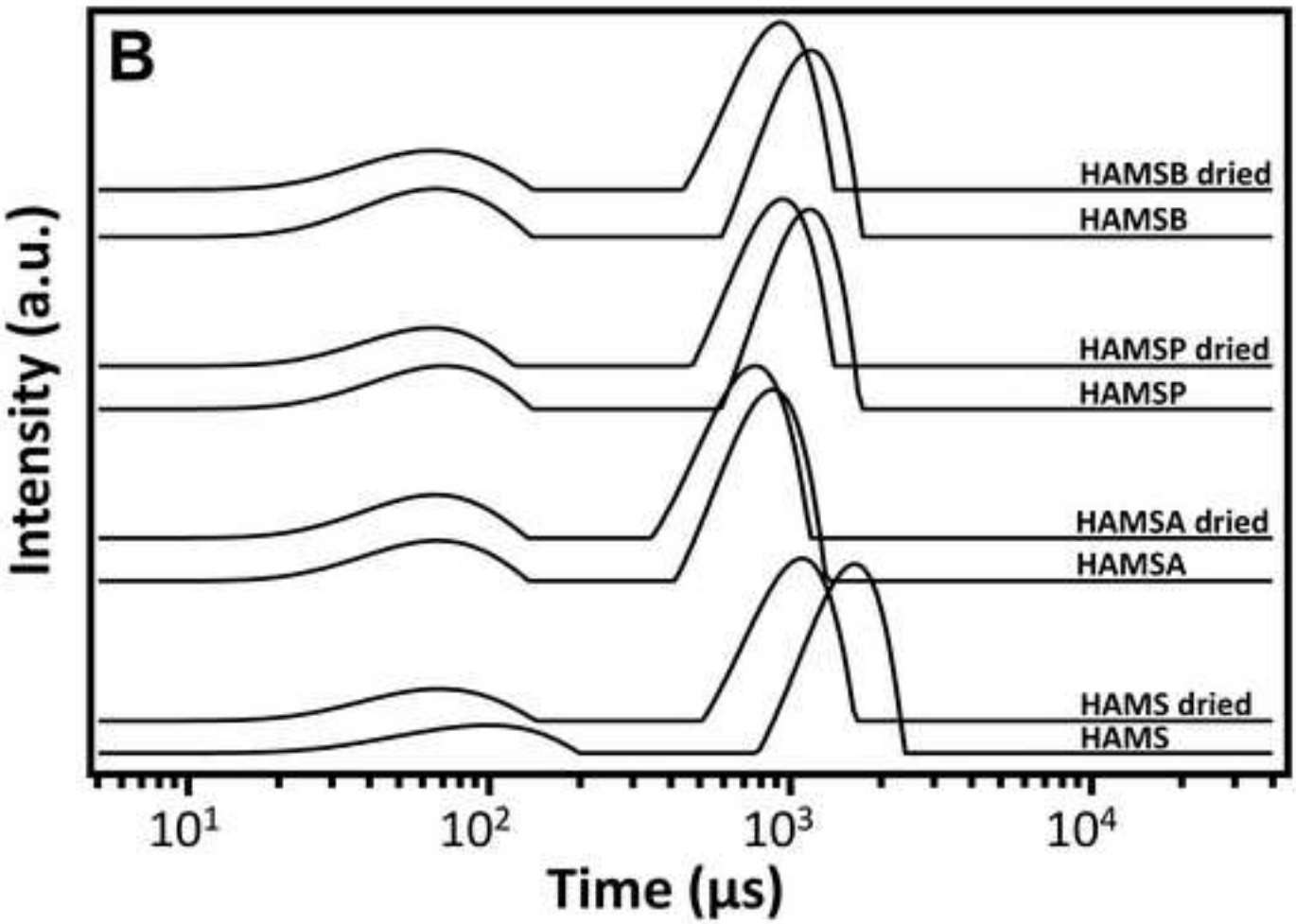

Figure 5

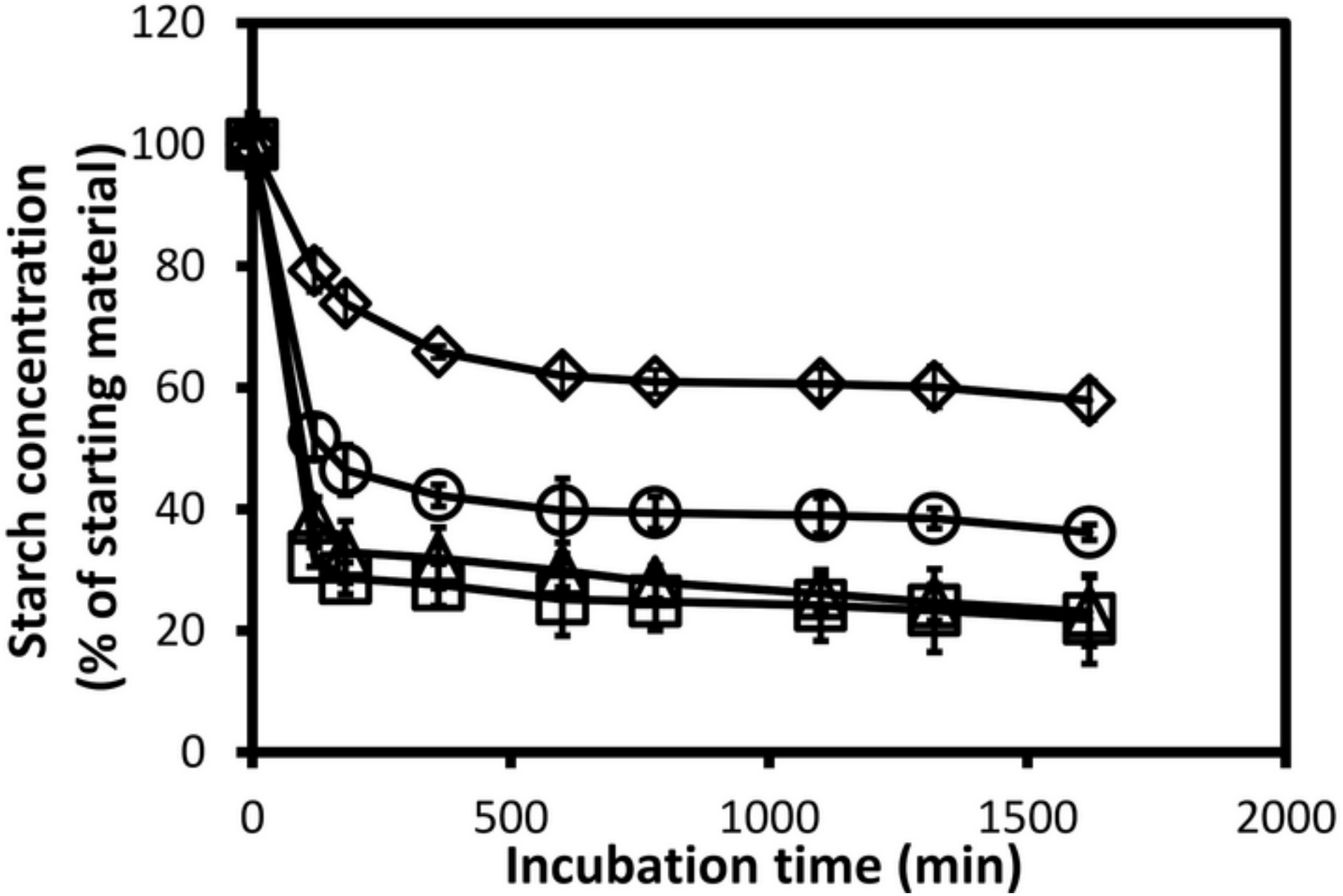
120
100
80
60
40
20
0
Starch concentration
(% of starting material)
0
500
1000
1500
2000
Incubation time (min)

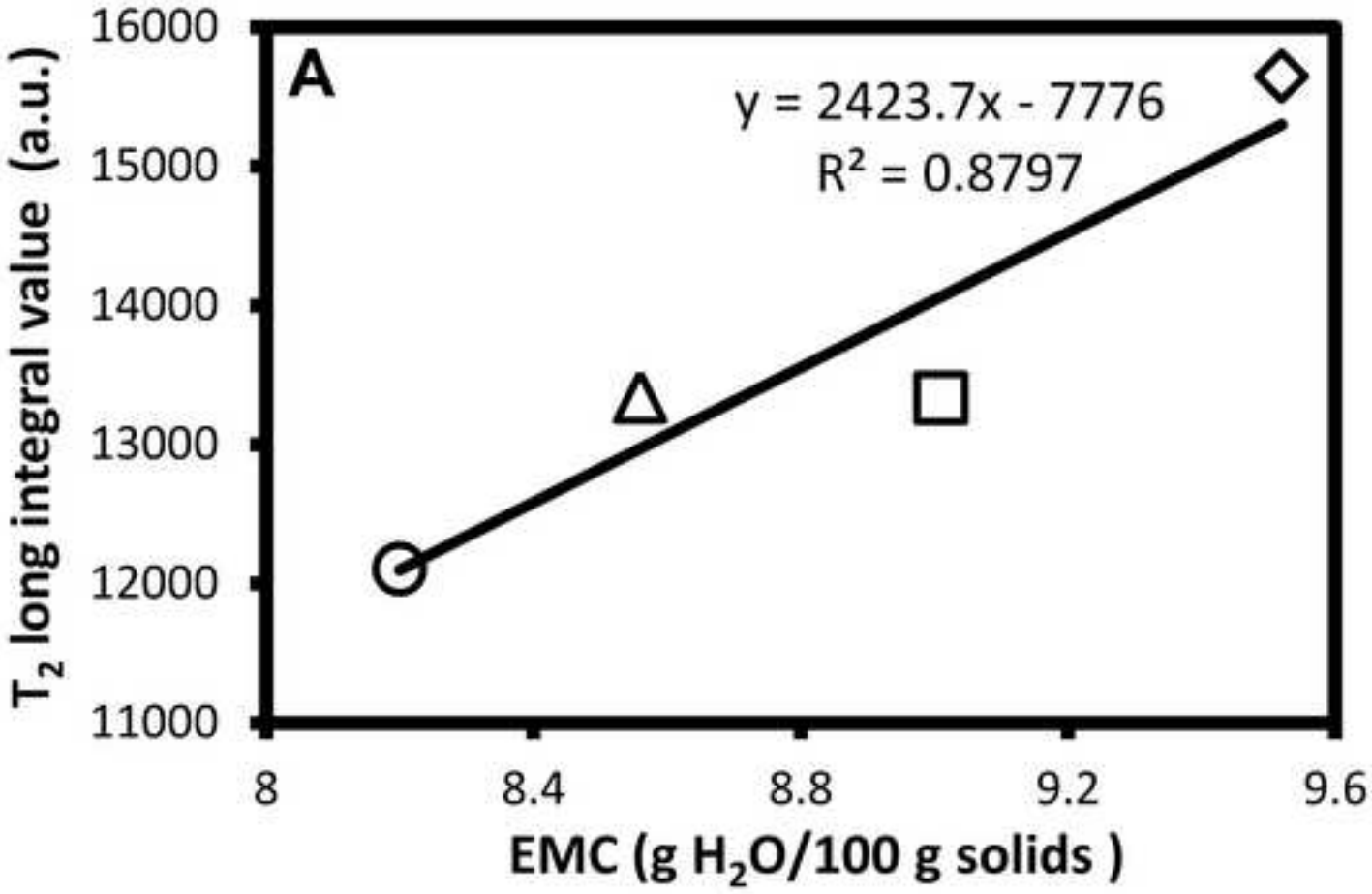

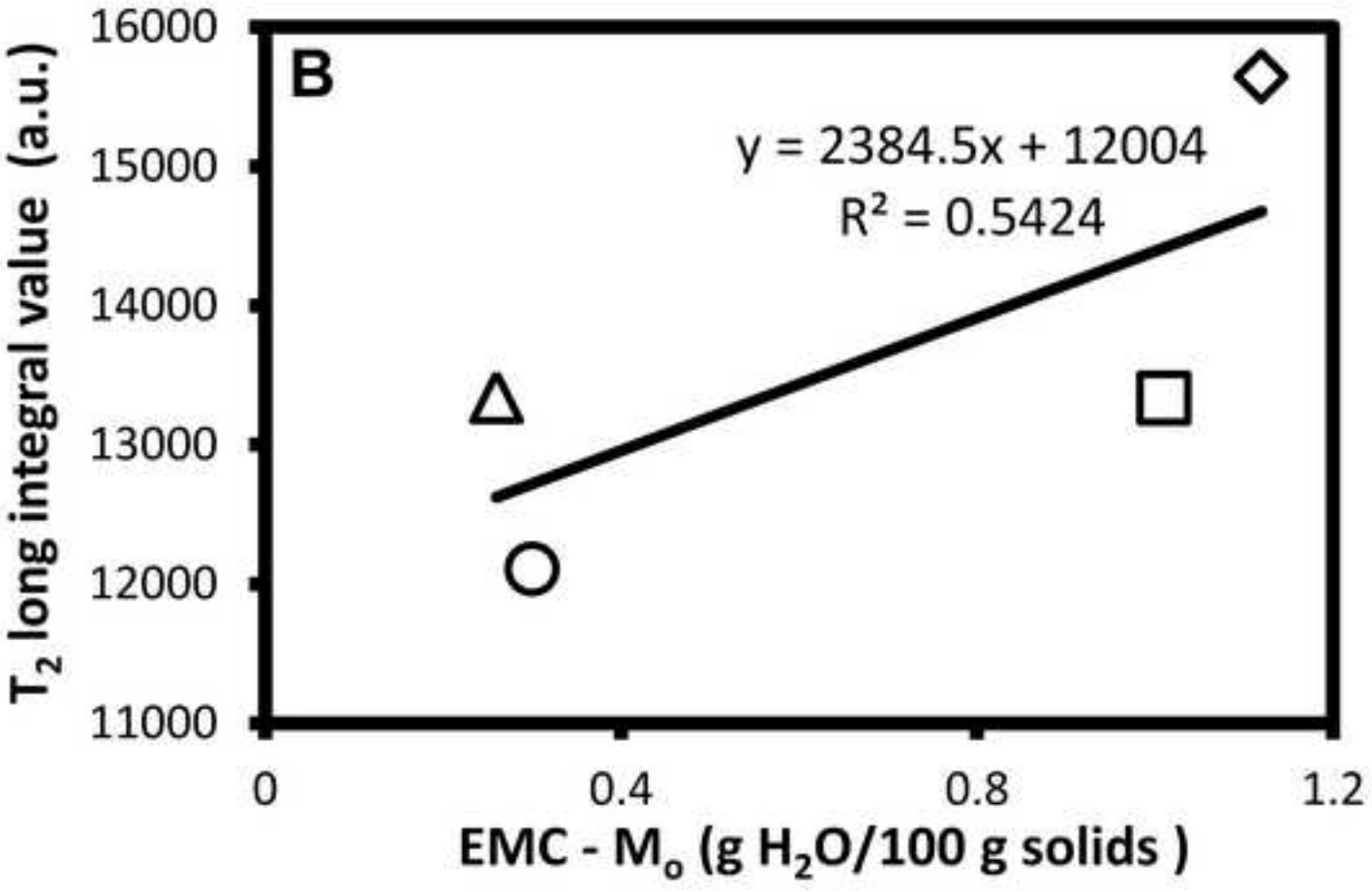

Author/s:
Lim, Y-M; Hoobin, P; Ying, D; Burgar, I; Gooley, PR; Augustin, MA

Title:
Physical characterisation of high amylose maize starch and acylated high amylose maize starches

Date:
2015-03-06

Citation:
Lim, Y. -M., Hoobin, P., Ying, D., Burgar, I., Gooley, P. R. & Augustin, M. A. (2015). Physical characterisation of high amylose maize starch and acylated high amylose maize starches. CARBOHYDRATE POLYMERS, 117, pp.279-285. https://doi.org/10.1016/j.carbpol.2014.09.068.